Chapter 2 THEORETICAL METHODOLOGY

"This chapter outlines the theoretical framework used for calculating a variety of cross-sections (CSs) for the atomic and molecular system. Here, we adopted two methodologies for the ionization threshold to the 5 keV impact energy range. We applied the Spherical Complex Optical Potential (SCOP) to estimate total cross-sections. For ionization and excitation CSs, we utilized the Complex Scattering Potential Ionization Contribution (CSP-ic) method. Furthermore, a newly established 2 parameters Semi empirical method (2p-SEM) to find out total and elastic cross sections. We will describe all the approximations which we have used in these methodologies".

2.1 Introduction

The study of electron collision phenomena holds enormous importance in the working of molecular physics, as well as its relevance in other scientific disciplines including chemistry, plasma science, astrochemistry and material science. ***Chapter 1*** provides a concise overview of the current landscape of molecular physics, which subsequently highlights the vital importance of conducting calculations pertaining to diverse cross sections (CSs) for electron induced processes associated with molecular targets. In the computation, our aim is to calculate total elastic, inelastic, ionization, and excitation CSs. Ionization CSs are complicated to extract directly, so our group has developed a method to compute from the total inelastic CSs. We described this method as a "Complex Spherical Potential Ionization Contribution (CSP-ic)". Theoretically, we begin our calculations from the generation of "phase shifts" for the investigation of total elastic and inelastic CSs [1]. Let us discuss the relationship between the CSs and quantum mechanical parameter, which are useful to compute varieties of cross sections (CSs).

2.2 Potential scattering

The potential between incoming electron and target cloud depends on the distance. First, consider the non-relativistic electron scattering from the target system. In the context of these scattering interactions, numerous phenomena are conceptualized regarding the spatial separation between the incident electron and the target electron cloud.

For a spinless particle with mass "m" and a potential $V(\vec{r})$, the time-independent "Schrodinger wave equation (SWE)" [1] is given by

$$-\frac{\hbar^2}{2m}\nabla_r^2\Psi(\vec{r}) + V(\vec{r})\Psi(\vec{r}) = E\Psi(\vec{r}) \tag{2.1}$$

The effective potential of the target is given by $V(\vec{r})$. $E = \frac{p^2}{2m}$ is the incident K.E., and the momentum "$p = \hbar k$", where "*k* is wave vector". In this theory, it is assumed that the potential is short-range and spherically symmetric. So, that $V(r) \rightarrow 0$ as $r \rightarrow \infty$ faster than any inverse power of *r*. By using the reduced potential equation 2.1 can be written as

$$\left[\nabla_r^2 + k^2 - U(r)\right]\Psi(\vec{r}) = 0 \tag{2.2}$$

$U(r) = \frac{2m}{\hbar^2} V(r)$ called as "reduced potential" in equation 2.2.

It is assumed that as $r \to \infty$, the potential diminishes more rapidly than 1/r, which ensures that the asymptotic boundary condition of the outgoing wave function is satisfied. The total wave function is expressed as,

$$\Psi_{k_i}^{(+)}(\vec{r}) \to A\left[e^{(ik_i \cdot r)} + f(\theta, \emptyset)\frac{\exp(ikr)}{r}\right] \text{ for } r \to \infty \tag{2.3}$$

Here, "*A"* represents the normalization factor, which is independent of the θ and ϕ, while *f(θ, ϕ)* is the angular function called 'scattering amplitude' satisfies above eq. 2.3 while *V(r)*, the potential is neglected at long distance. The first term in eq. 2.3, $e^{(ik_i \cdot r)}$ represents the incident plane wave and the other term represents the outgoing spherical waves.

2.2.1 Partial wave analysis

This assumes the spherically symmetric potential, which allows us to focus exclusively on the radial portion of the equation 2.1. The "Partial wave analysis (PWA)" is essentially a method for expanding angular momentum[1,2]. In this, the scattering wave function is expressed as a series of partial wave components, each corresponding to a specific angular momentum quantum number. The PWA is employed to obtain the "complex phase shifts $\delta_l(k)$" for each orbital angular momentum, "l" [2], then it is employed in order to compute total CSs. It is merely an angular momentum emergence approach [2]. So, the wave function is written in terms of "l" and "m", orbital and magnetic quantum numbers, respectively.

$$\Psi_{k_i}^{(+)}(k,r) = \sum_{l=0}^{\infty} \sum_{m=-1}^{+1} C_{lm}(k) R_{lm}(k,r) Y_{lm}(\theta,\phi) \tag{2.4}$$

The term $R_{lm}(k,r)$ is the radial component and thus the radial SWE is expressed as,

$$-\frac{\hbar^2}{2m}\left[\frac{1}{r^2}\frac{d}{dr}\left(r^2\frac{d}{dr}\right) - \frac{l(l+1)}{r^2}\right] R_l(k,r) + V(r) R_l(k,r) = E R_l(k,r) \tag{2.5}$$

By substituting the value of $R_l(k,r) = \frac{u_l(k,r)}{r}$ and U(r) with asymptotic Bessel functions, we get,

$$u_l(k,r) \to A_l(k) \sin\left[kr - \frac{1}{2}l\pi + \delta_l(k)\right] \text{ for large } r \tag{2.6}$$

Complex phase shifts $\delta_l(k)$ are quantitatively computed with the use of $rR_l(k,r) = u_l(k,r)$.

Let's move on to solving the radial eq. 2.5 for region, $r < a$, where " a " denotes the finite range of potential scattering. The boundary condition requires that, the radial waves R_l, and $\mathrm{R}_l^{-1}\frac{dR_l}{dr}$ should be consistent at $r = a$.

Therefore, at $r = a$, we get,

$$R_l(k,r) = \hat{A}_l(k)[j_l(k,r) - \tan\ \delta_l(k)\eta_l(k,r)]_{r=a} \tag{2.7}$$

$$\gamma_l(k) = \frac{k[j_l'(ka) - \tan\ \delta_l(k)\eta_l'(ka)]}{j_l(ka) - \tan\ \delta_l(k)\eta_l(ka)} \tag{2.8}$$

Where, η_l and j_l are the Neumann and Bessel functions. The term η_l' and j_l' indicate a derivation with respect to ' r '.

Hence,

$$\tan\ \delta_l(k) = \frac{kj_l'(ka) - \gamma_l(k)j_l(ka)}{k\eta_l'(ka) - \gamma_l(k)\eta_l(ka)} \tag{2.9}$$

Using above eq., $\delta_l(k)$ can be calculated.

Computation of scattering amplitude, $f(k,\theta)$ can be done through,

$$f(k,\theta) = \frac{1}{2ik}\sum_{l=0}^{\infty}(2l+1)[\exp\{2i\delta_l(k)\} - 1]P_l(\cos\ \theta) \tag{2.10}$$

Equation 2.10 could be modified as,

$$f(k,\theta) = \frac{1}{2ik}\sum_{l=0}^{\infty}(2l+1)[S_l(k) - 1]P_l(\cos\ \theta) \tag{2.11}$$

$S_l(k) = \exp\{(2i\delta_l(k)\}$ is called S-matrix component. Hence, obtaining the scattering amplitude is made achievable by knowing phase shifts. Eq. 2.11 can be modified as

$$f(k,\theta) = \frac{1}{k}\sum_{l=0}^{\infty}(2l+1)\exp(i\delta_l)\sin\ \delta_l P_l(\cos\ \theta) \tag{2.12}$$

Differential CSs can be computed from $f(k,\theta)$ through,

$$\frac{d\sigma}{d\Omega}(k,\theta) = |f(k,\theta)|^2$$

Through the interaction potential $V(\mathrm{r})$, elastic scattering can be obtained

$$\frac{d\sigma}{d\Omega}(k,\theta) = \frac{1}{k^2}\sum_{l=0}^{\infty}\sum_{V=0}^{\infty}(2l+1)(2l'+1)\exp\ \mathrm{i}(\delta_l - \delta_V) \times \sin\ \delta_l \sin\ \delta_V P_l(\cos\ \theta)P_V(\cos\ \theta) \tag{2.13}$$

Total CSs may be obtained through,

$$\sigma_{tot}(k) = \frac{4\pi}{k^2}\sum_{l=0}^{\infty}(2l+1)\sin^2\ \delta_l(k) = \sum_{l=0}^{\infty}\sigma_l(k) \tag{2.14}$$

All partial wave $\sigma_l(k)$ is shown as follows:

$$\sigma_l(k) = \frac{4\pi}{k^2}(2l+1)\sin^2\delta_l(k) \tag{2.15}$$

When the $\sin^2\ \delta_l(k) = 1$

$$\sigma_l^{\max}(k) = \frac{4\pi}{k^2}(2l+1) \tag{2.16}$$

$$\delta_l(k) = \left(n + \frac{1}{2}\right)\pi \text{ with } n = 0, \pm 1, \pm 2 \ldots \tag{2.17}$$

We can analyse the asymptotic behaviour of the wave function as a combination of scattered spherical wave $e^{(ikr)}$ & the incident plane wave $e^{(-ikr)}$.

$$\Psi_{ki}^{(+)}(k,r) \underset{r\to\infty}{\longrightarrow} A(k)\sum_{l=0}^{\infty}(2l+1)i^l\frac{i}{2kr}\exp(i\delta_l) \times \left[(-1^l)e^{-ikr} - S_l e^{ikr}\right]P_l(\cos\ \theta) \tag{2.18}$$

$S_l = e^{(2i\delta_l)}$ in this case. δ_l is considered valid in cases involving only elastic processes, where $|S_l| = 1$; however, it is necessary to extend the framework to account for nonelastic processes as well. In order to adequately address elastic phenomena within the

framework of 'absorption' δ_l must be complex. This necessity arises from the fact that the amplitude of the transmitted radial wave may diminish in the presence of inelastic processes or maintain its constancy in scenarios where only elastic scattering takes place, thereby suggesting that

$$|S_l| \leq 1 \tag{2.19}$$

As an outcome, we implement a significant phase shift.

$$\delta_l = R_e\delta_l + iI_m\delta_l \tag{2.20}$$

As a result, the intricate S-matrix is characterized by,

$$S_l = \exp\left[2i(R_e\delta_l + iI_m\delta_l)\right] \tag{2.21}$$

That is to say,

$$S_l = \eta_l \exp\left(2iR_e\delta_l\right) \tag{2.22}$$

Where "inelasticity" or "absorption factor" is described as $\eta_l = \exp\left(-2I_m\delta_l\right)$. The elimination of particles from the event channel is characterised in this context as "absorption."

We have $|S_l| \leq 1$ as,

$$0 \leq \eta_l \leq 1$$

And

$$I_m\delta_l \geq 0.$$

For pure elastic collision,

$$\eta_l = 1 \text{ (i.e., } I_m\delta_l = 0).$$

2.2.2 Optical theorem

In the process of calculating the particle flux, we have not considered role of forward scattering, wherein particles are scattered in the same direction as the incident electron beam. Now, let us endeavour to comprehend what happens in the situation where θ = 0. The equation 2.10 yields the scattering amplitude, which is expressed as

$$f(k,\theta) = \frac{1}{k}\sum_{l=0}^{\infty}(2l+1)\exp(i\delta_l)\sin\delta_l P_l(\cos\theta) \tag{2.23}$$

At θ = 0, $P_l\ (cos\ \theta) = 1$.

Thus,

$$f(k,0) = \frac{1}{k}\sum_{k=0}^{\infty}(2l+1)[\cos\delta_l + i\sin\delta_l]\sin\delta_l \tag{2.24}$$

So, imaginary part is derived by,

$$\text{Im}\ f(k,0) = \frac{1}{k}\sum_{l=0}^{\infty}(2l+1)\sin^2\delta_l \tag{2.25}$$

and the total CSs from equation (2.14) as,

$$\sigma(k) = \frac{4\pi}{k^2}\sum_{l=0}^{\infty}(2l+1)\sin^2\delta_l(k) \tag{2.26}$$

Comparing equation (2.14) and (2.26),

$$\sigma(k) = \frac{4\pi}{k^2}\,\text{Im}\ f(k,\theta=0) \tag{2.27}$$

Above expression is refereed as ‘optical theorem’. The aforementioned relationship arises as a straight away from flux probability conservation. This phenomenon arises as a result of the destructive interference that takes place between the incoming and scattered wave in “forward

region (θ = 0)". In other words, the imaginary component of the forward scattering indicates the attenuation of intensity. The title "Optical Theorem" refers to the understanding of this concept through an optical analogy.

2.3 SCOP: Spherical Complex Optical Potential

The main objective is to construct a simple theory with the approximation which allows for estimation of the cross sections within the experimental uncertainty. In this we have focused with the target system in their ground state, which results in elastic effect as well as inelastic effect within the present energy range (from IP to 5 KeV). In the computation of CSs idea of the complex phase shift has been developed due to the absorption process in the presence of absorption potential and we will deal with this complex potential which is termed "complex optical potential".

The "complex optical potential" is defined as

$$V_{opt} = V_R + iV_I \tag{2.28}$$

The above equation 2.28 contains the optical potential's real and imaginary parts respectively and E_i is the incident particle energy. The real portion contains static (V_{st}), exchange (V_{ex}), and polarization (V_{pol}) terms and the imaginary part contains absorption (V_{abs}) term. These model potentials are useful to understand the interactions between incoming electrons and molecular target systems.

2.3.1 Target charge density

Accurately calculating the charge density of larger atoms is challenging, so we need to employ the use of approximation methods. To determine the static charge density, we utilize wave functions calculated through "Roothan-Hartree-Fock (RHF)", which are represented by "Slater Type Orbitals". This approach, as underline in the work of Clementi & Roetti [3], provides a practical way to approximate charge densities for heavier atoms. Bunge and coworkers [4] tabulated very precise versions of RHF. The RHF wave functions R_{nl} are expanded as,

$$R_{nl} = \sum_{j} S_{jl} C_{jln} \tag{2.29}$$

The parameters of these RHF wave functions are based on ground-state atoms. Here, S_{jl} is the STOs and C_{jnl} are the orbital expansion factors. S_{jl} is given as,

$$S_{jl} = N_{jl} r^{n_{jl}-1} \exp\left(-Z_{jl} r\right) \tag{2.30}$$

With the normalization factor, N_{jl},

$$N_{jl} = \frac{\left(2Z_{jl}\right)^{\left[n_{jl}+\frac{1}{2}\right]}}{\sqrt{(2n_{jl})!}} \tag{2.31}$$

The parameters are n_{jl} (principal quantum number), Z_{jl} (orbital exponent), l (azimuthal quantum number). We can compute electronic charge density using C_{jnl}, Z_{jl} tabulated by Bunge *et al* [4]. Let us now use these values to derive the charge density of atomic oxygen. By using the eq. (2.29), (2.30), (2.31) the R_{nl} wave functions for electrons in individual orbital R_{1s}, R_{2s}, R_{2p}, & R_{3s} can be obtained.

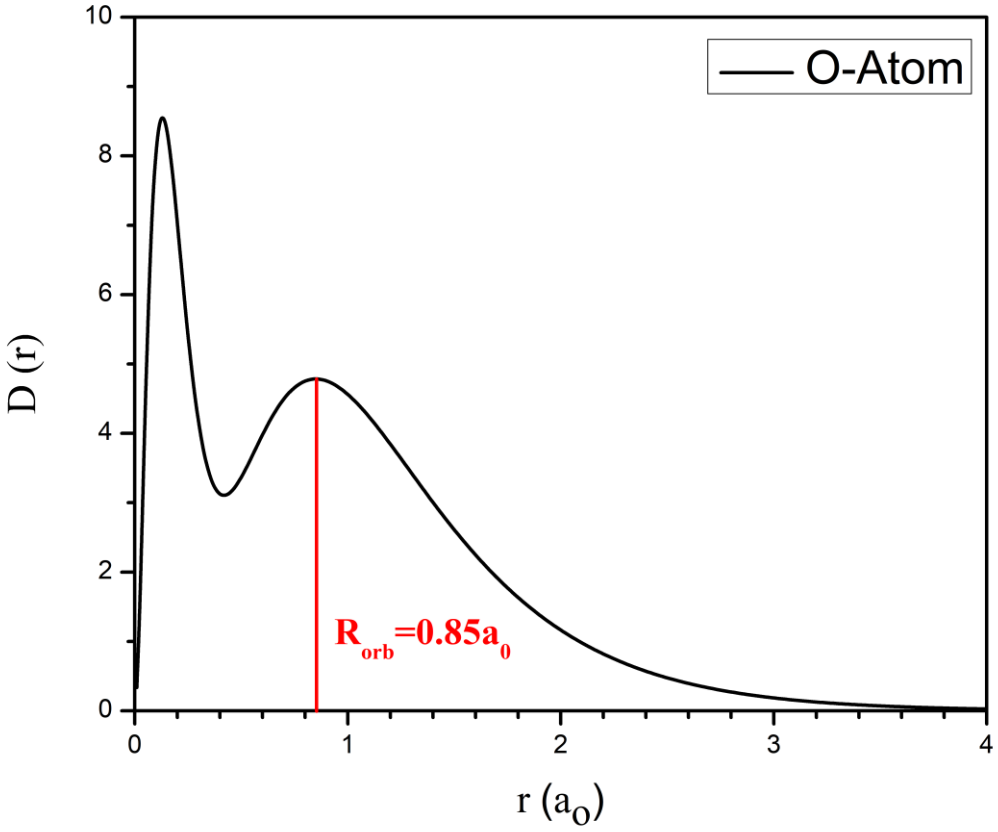

Figure 2.1 Charge density

$$\rho(r)=\frac{1}{4\pi}\left[2\left|R_{1s}\right|^2+2\left|R_{2s}\right|^2+6\left|R_{2p}\right|^2+\left|R_{3s}\right|^2\right] \tag{2.32}$$

Here, $4\pi\int_0^\infty \rho(r)r^2dr = Z$. In fig. 2.1, the resultant radial charge density (*D(r)*) for the oxygen atom and also it shows two distinct peaks, for n = 1 and 2. The peak (R_{orb} = orbital radius) is detected at $0.85a_0$. The method of least squares was employed to optimize the D(r) equation pertaining to the radial distribution of electrons in the renowned research conducted by Cox and Bonham [5].

The analytical calculation of charge density is done through,

$$\rho(r) = \frac{Z}{4\pi r}\sum_{i=1}^{n} \gamma_i \lambda_i^2 \exp(-\lambda_i r) \qquad (2.33)$$

Where γ_i and λ_i are field-dependent Cox and Bonham variables [5], some of them are listed below.

Table 2.1 γ_i and λ_i for Hydrogen and Carbon

Hydrogen (Z=1)		**Carbon (Z=6)**	
γ_i	**λ_i**	**γ_i**	**λ_i**
0.0524	1.9986	1.2820	1.9147
5.036	1.8954	-0.0616	43.9979
-4.0876	2.1161	4.2766	5.3154
		6.7513	15.9205
		-3.9495	4.1654
		-7.3000	15.0304

Table 2.2 γ_i and λ_i for Oxygen and Fluorine

Oxygen (Z=8)		**Fluorine (Z=9)**	
γ_i	**λ_i**	**γ_i**	**λ_i**
1.3017	2.2491	1.2644	2.4893
-0.167	19.5541	-0.1763	21.5801
2.6221	6.9101	3.0409	8.2525
1.5881	10.7798	1.4796	13.0569
-2.8644	6.056	-3.1755	7.3313
-1.4804	9.9776	-1.4335	12.2279

Table 2.3 γ_i and λ_i for Nitrogen

Nitrogen (Z=7)	
γ_i	**λ_i**

1.3678	2.0273
-0.238	16.5256
2.8625	5.9953
1.9402	9.9313
-3.0396	5.0882
-1.8916	9.0839

2.3.2 The static potential

The electrostatic potential experienced by the unperturbed target charge distribution when an incoming electron approach is represented by the static potential (V_{st}). This potential, $V_{st}(r)$ is characterised at a distance "r" using the [6], Poisson's formula.

At a distance 'r' the potential value is determine by poisson's equation given by

$$V_{st}(r) = -\frac{Z}{r} + 4\pi\left[\frac{1}{r}\int_0^r \rho(r')r'^2 dr' + \int_r^\infty \rho(r')r' dr'\right] \tag{2.34}$$

Where Z represents the "atomic number" and $\rho(r')$ denotes "charge density" of the target. Consider the hydrogen atom (Z=1), we obtain a precise static potential equation as

$$V_{st}(r) = -\left(1 + \frac{1}{r}\right)e^{(-2r)} \tag{2.35}$$

Above equation 2.35 is the real potential and only acts at short range. It is very difficult to establish an accurate solution for the "static potential" and "charge density" in heavier atoms, we must rely on approximation methods. The static potential calculated by Cox and Bonham [5] represented an analytical expression by using the summation of Yukawa terms beginning from "Hartree-Fock" and the relativistic wave functions for all neutral atoms. This analytical formula is given as

$$V_{st}(r) = -\frac{Z}{r}\sum_{i=1}^{n} \gamma_i \exp(-\lambda_i r) \tag{2.36}$$

The modified version of the RHF wave function is known as the “Dirac Hartree Fock Slater (DHFS)” was introduced by the Salvat and coworkers [7] which accounts for the relativistic effects. The static potential accurately fits in this method and the approximation relies on the variables for the atomic screening function, determined via Dirac Hartree Fock Slater data. The static potential analytic expression is given by

$$V_{st}(r) = -\frac{Z}{r}\sum_{i=1}^{n} A_i \exp\left(-\alpha_i r\right) \tag{2.37}$$

Here, “A_i” and “α_i” represent the atomic screening variables [6]. In the current work, we have calculated charge densities & potentials for lighter atoms through analytical formula of Cox and Bonham [5].

2.3.3 The exchange potential

The additional component in the optical potential relates to the exchange interaction that occurs when an incident electron swaps places with an electron in the target. “Hara” [8] adopted the “free electron gas exchange model” to account for the “exchange effect”. He considered the electron gas as a Fermi gas composed of non interacting electrons, ensuring that the overall wave function was anti-symmetrized in accordance with the “Pauli exclusion principle”. The expression of the “exchange potential” is written as,

$$V_{ex}(r,k) = -\frac{2}{\pi}k_F\left[\frac{1}{2} + \frac{1-\eta^2}{4\eta}\ln\left|\frac{1+\eta}{1-\eta}\right|\right] \tag{2.38}$$

Where,

$$\eta = \frac{\sqrt{k^2 + k_F^2 + 2I}}{k_F} \tag{2.39}$$

$$k_F = \sqrt[3]{3\pi^2\rho(r)}\text{ , fermi wave vector} \tag{2.40}$$

The aforementioned model is called the "Hara Free Electron Gas Exchange (HFEGE)" model. *I* (in Hartree unit) denote the ionization energy which is referred to as the minimum amount of energy needed to liberate bound state electron. Here, the kinetic energy of electron in the asymptotic region is given by $E + I$, according to the approximation in the numerator of equation 2.40. However, for large r, it is obvious to correct the behavior by removing *I*.

This approximation is called the "Asymptotically Adjusted" is written as,

$$\eta = \frac{\sqrt{k^2 + k_F^2}}{k_F} \tag{2.41}$$

In the investigation of atoms or molecules with open shell configurations, we use the "exchange potential" as given in equation (2.38) and for the closed shells, and it is available in the prior work of "Riley and Truhlar" [9].

$$V_{ex}(r,k) = \frac{1}{2}\left[E_D - \sqrt{E_D^2 + 4\pi\rho(r)}\right] \tag{2.42}$$

The local kinetic energy is denoted by E_D and it is written as

$$E_D = \frac{1}{2}k_i^2 - V_{st} \tag{2.43}$$

2.3.4 The polarization potential

When an approaching electron collides with atoms or molecules, it causes a distortion in the electron cloud. This effect is highly notable due to the resultant multipole moments. The polarization potential is inherently attractive and holds substantial importance. This effect will provide the additional term in the potential which is called "polarization potential" in the formula for potential energy [1]. The asymptotic region is given by

$$V_{pol} = -\frac{\alpha_d}{2r^4} - \frac{\alpha_q}{2r^6} \tag{2.44}$$

In this context, the contributions from higher-order multipolar terms are dismissed. In equation (2.44), α_d and α_q are the static polarizabilities corresponding to the dipole and quadrupole of the target compound, respectively.

This potential exhibits an attractive, long-distance characteristic and changes asymptotically as r^{-4} at r approaches infinity. At "r = 0", there is a singularity and it can be avoided by introducing a cut-off parameter 'r_c' in equation (2.45) as follows,

$$V_{pol} = -\frac{\alpha_d}{2(r^2 + r_c^2)^2} \tag{2.45}$$

It is known as "Buckingham polarization potential" [10,11]. For the fast-incoming electron target electrons are just unable to respond. So, for high energies, we use the energy dependent or dynamic form for the polarization potential given by Khare and colleagues [12].

$$V_{dp}(r,k) = -\frac{1}{2}\left[\frac{\alpha_d r^2}{(r^2 + r_c^2)^3} + \frac{\alpha_q r^4}{(r^2 + r_c^2)^5}\right] \tag{2.46}$$

By using the "Born approximation" [1,13], we find that

$$r_c = \frac{3k}{8\Gamma} \tag{2.47}$$

Where " Γ " represents the average excitation energy of the atom. The straightforward behaviour of r^{-4} is not applicable at brief distances. Therefore, it is necessary to take into account the effects of electron correlation at these short ranges.

2.3.5 The absorption potential

The absorption potential described by Staszewska's quasi free and Pauli blocking model relies on the T_{loc} and the $\rho(r)$ charge density expressed in units of angstrom, as follows:

$$V_{abs} = -\frac{1}{2}\rho(r) v_{loc} \sigma_{ee} \tag{2.48}$$

In this scenario, the local speed of electron is denoted by v_{loc}, and the total CSs of the interaction between target electron and incoming particles are denoted by σ_{ee}.

A non-empirical formula [18] as may be used to rewrite,

$$V_{abs}(r, E_i) = -\rho(r)\left(\frac{T_{loc}}{2}\right)^{\frac{1}{2}} \times \left(\frac{8\pi}{10k_F^3 E_i}\right)\theta(p^2 - k_F^2 - 2\Delta)\cdot(A_1 + A_2 + A_3) \quad (2.49)$$

The definition of the dynamical components A_1, A_2 and A_3 in the expression above is,

$$A_1 = \frac{5k_F^3}{2\Delta};$$

$$A_2 = \frac{k_F^3(5p^2 - 3k_F^2)}{(p^2 - k_F^2)^2};\ \text{and} \quad (2.50)$$

$$A_3 = 2\theta(2k_F^2 + 2\Delta - p^2)\frac{(2k_F^2 + 2\Delta - p^2)^{\frac{5}{2}}}{(p^2 - k_F^2)^2}$$

Here, p^2 is $2\mathrm{E_i}$ $(Hartree)$, incident energy and $\theta(x)$ is Heavyside step-function. T_{loc} is an illustration of the local kinetic energy of the incident electron and is

$$T_{loc} = E_i - V_R = E_i - (V_{ex} + V_{st}) \quad (2.51)$$

As the V_{abs} is insensitive to long range and only affects short-range, it is disregarded in T_{loc}. In contrast to kinematics, the absorption potential is influenced by the target's energy-dependent variable, $\rho(r)$, and the charge density of its molecules, Δ.

The energy value in the exclusive model [18] creates a threshold beyond which the inelastic channel, with absorption potential $V_{abs} = 0$, is energetically prevented. The first, Staszeweska concept [18] Δ accounts for the target's ionization threshold for all incident energies. Therefore, the discrete excitation contributions at lower incidence energy are essentially ignored. This was earlier recognized by Blanco and Garcia [19], and they talked about the need for Δ value. We

modified the parameter to account for the inelastic channel linked to excitations at various levels of E_i, corresponding to the ionization threshold (I) of the target. For that progressively approaches its peak value equal to (I), the lowest quantity is provided. As a result, the variable amount that explains a greater portion of the absorption potential in the charge-cloud region of the target [19], is represented as,

$$\Delta(\mathrm{E_i}) = \eta I + \beta(E_i - IP) \tag{2.52}$$

The contribution of discrete excitations below the ionization threshold to Δ is accounted for by the first term in equation 2.52, which corresponds to the minimum value of Δ at $E_i = IP$. The energy dependence on Δ prior to reaching its maximum value, I, is represented by the second term. At the energy E_p, the inelastic CSs reach their peak. The variable β is subsequently estimated by the condition using $\Delta = IP$ at $E_i \geq E_P$.

To figure out the proportion η at $E_i = IP$, we may aggregate all individual energy levels under I plus the continuum I to get the total electrical excitations from the onset to its continuity I. Thus, the proportion of the total contribution from all discrete excitation channels to the overall contribution from all channels, including the continuum, can be represented as,

$$\eta = \frac{\sum_{n=1}^{n_\infty - 1} E_n}{\sum_{n=1}^{n_\infty} E_n} = \left(1 - \frac{\mathrm{I}}{\sum_{n=1}^{n_\infty} E_n}\right) \tag{2.53}$$

In this context, E_n denotes the electron energy of n^{th} state , where n_∞ indicating continuum.

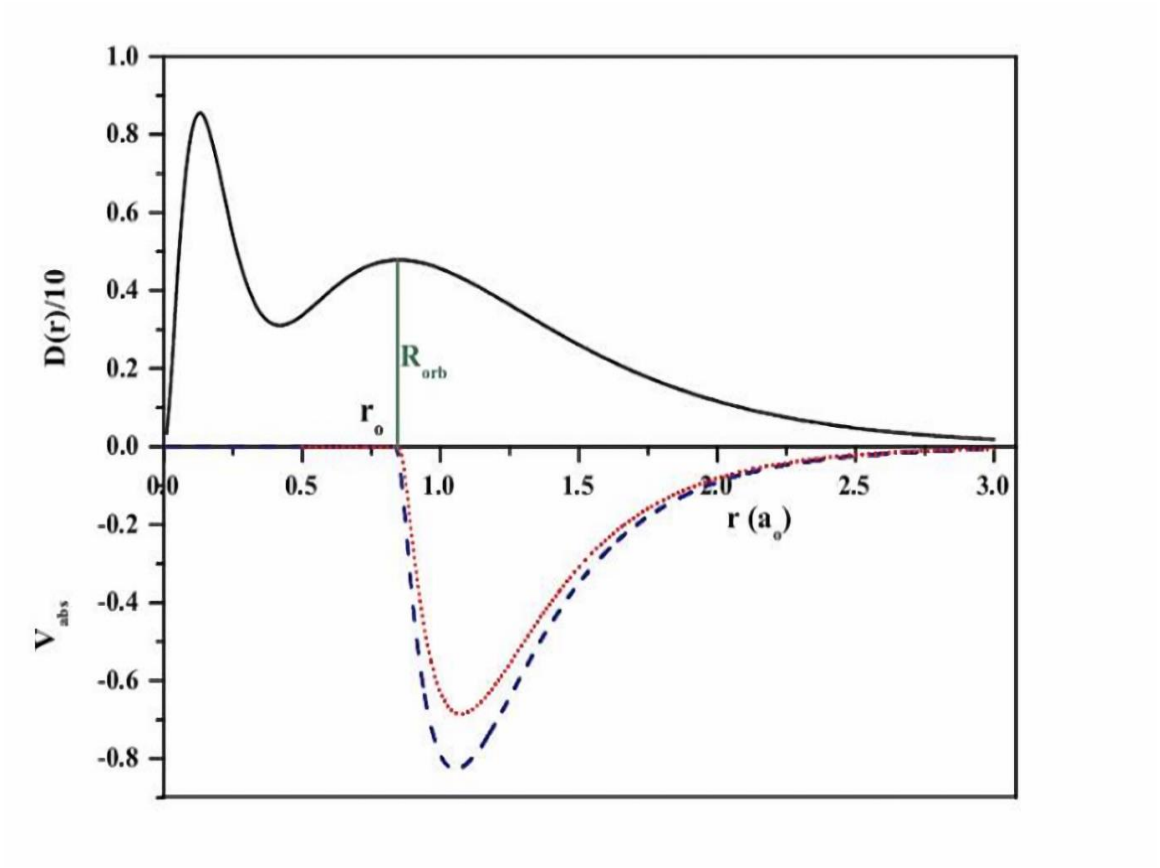

Figure 2.2 V_{abs} for O-atom at 100 eV

Dash: V_{abs} : $\Delta = IP$ =13.60 eV; Solid: $\frac{D(r)}{10}$; Dot: V_{abs}: $\Delta = IP$ =15.07 eV

For example, the starting value of this attractive potential at 100 eV is $0.85a_0$, as illustrated in figure 2.2, concerning the O-atom. In the aforementioned figure 2.2, the charge distribution $D(r) = 4\pi r^2 \rho(r)$ is presented for comparison purposes. The impact energy at 500 eV, the value is established at $0.25\ a_0$ (not depicted in figure 2.2).

The outcome is in higher values of Q_{inel} , a somewhat more loss of scattered flux into inelastic pathways. The avoidance of certain features in the V_{abs}, such as varying transition possibilities for various states are also partially to blame for this.

The inner electronic shells, which are more difficult to excite or ionize, are also penetrated by the potential V_{abs}. However, this absorption potential has a general predictive capacity and excellent analytical capabilities. As a result, it must be rectified using $\Delta \geq I$ in order to be used at medium energies.

Consequently, we select the Δ parameter to be a smoothly changing function of E_i close to the IP value. As energy levels increase, the potential V_{abs} and the Q_{inel} diminish in intensity.

In illustration 2.2, we present a graphical representation of the "radial charge density" of the target, indicated as $4\pi r^2\rho(r)$, along with V_{abs} for two scenarios: (i) where $\Delta = I$, (ii) Δ is treated as continuous variable around IP.

$$\Delta(E_i) = \Delta_{min} + \beta(E_i - \Delta_{max}) \tag{2.54}$$

Equation 2.54 yields the parameter β as $\Delta = I + 1$ (eV) at$E_i = E_P$, with Δ remaining constant thereafter.

2.4 CSP-ic: Complex Spherical Potential- ionization contribution

The study of electron interactions, two CSs are dominant for many potential applications: Total CSs (Q_T) and Ionization CSs (Q_{ion}). However, accurately calculating Q_{ion} from Q_T has been a challenge. To address this, we have semi-empirical method is called "Complex Scattering Potential - ionization contribution (CSP-ic)" [21] has been developed. Unlike traditional approaches like BEB [22] and DM [23], which calculate Q_{ion} by summing up contributions from individual electron shells, CSP-ic takes a different route. It cleverly utilizes the total inelastic CSs (Q_{inel}), which includes all possible energy-loss processes, both ionization and excitation. This unique approach not only provides Q_{ion} but also inherently accounts for all the discrete and continuous inelastic processes, offering a more complete picture of electron collision dynamics. Total inelastic CSs includes total ionization CSs and another noteworthy contribution from allowed excitation CSs denoted by $(\sum Q_{exc})$. The overall inelastic CSs encompass both the total ionization CSs and an additional significant component that collectively contributes to the total electronic excitation $(\sum Q_{exc})$ CSs.

$$Q_{\text{inel}}(E_i) = \sum Q_{\text{exc}}(E_i) + Q_{\text{ion}}(E_i) \tag{2.55}$$

The first term shows aloe allowed excitation CSs for possible electronic channels in expression 2.55, whereas the subsequent part reflects all ionization processes into continuum [24].

An important discrepancy that serves as the foundation for the CSP-ic methodology is shown in the following expression.

$$Q_{\text{inel}}(E_i) \geq Q_{\text{ion}}(E_i) \tag{2.56}$$

The CSP-ic formalism is a semiempirical procedure developed by us to compute Q_{ion} from Q_{inel} through the dynamic ratio, which is given below

$$R(E_i) = \frac{Q_{\text{ion}}(E_i)}{Q_{\text{inel}}(E_i)} \tag{2.57}$$

It is so, $0 \leq R \leq 1$. In the expression 2.58, we need $R = 0$, when incident energy (E_i) is less then equal to IP. It is noticed that, in accordance with the general experimental trend, the ratio R rises gradually as the energy rises above the threshold.

$$R(E_i)\begin{cases} = 0 & \text{for} \quad E_i \leq I \\ = R_P & \text{at} \quad E_i = E_P \\ \cong 1 & \text{for} \quad E_i > E_P \end{cases} \tag{2.58}$$
$$\tag{2.59}$$
$$\tag{2.60}$$

Here, E_P shows the impact energy at which the computed Qinel attains its highest value. The maximum value of Q_{inel} appears at incident energy at which Q_{ion} starts to reach to its peak and summed excitation CSs decrease. The equation 2.59, $R(E_i) = R_P$ is derived from experimental evidence, which shows that ionization contributes about 70-80% [25, 26] at the peak of the inelastic CSs. R_P represents the magnitude of R(E_i), at $E_i = E_P$, and it has been shown that, at $E_i = E_P$ the contribution of ionization is approximately 70 to 80%. This is considered through semi-empirical calculations.

Similarly, the second criterion is satisfied as well, since at higher energies, ionization processes dominate the inelastic scattering over excitation processes, causing the ratio to approach unity under these conditions. Although this introduces an uncertainty of approximately ±7% in the calculation of the direct ionization CSs, this is still smaller than the typical experimental uncertainty, which ranges from 10% to 15%. While choosing a variable ratio might seems that the method remains reliable and produces consistent results. Absolute determination of this ratio is challenging due to the lack of a standard procedure, and the value of R_P can vary

depending on the specific target system. Nonetheless, the selection of a ratio within the 0.7 to 0.8 range does not compromise the general applicability of the procedure. Ionization potentials varied from 8 to 14 eV for most of the targets explored in this investigation. The assigned R_p value is derived by considering that, as one exceeds the ionization potential value the ionization CSs begin to dominant, indicating their association with an infinite number of open scattering channels.

Since The actual significance of ratio R cannot be anticipated precisely, an iterative technique can be used. To derive Q_{ion} from Q_{inel}, we need dynamic R beyond the ionization potential ($E_i \geq I$). So, we present the dynamic ratio R as follow,

$$R(E_i) = 1 - f(U) \tag{2.61}$$

$$R(E_i) = 1 - \mathrm{C}_1 \left[\frac{C_2}{U + a} + \frac{\ln U}{U}\right] \tag{2.62}$$

With $\mathrm{U} = \frac{E_i}{I}$, U is dimensionless quantity.

The following consideration is used to determine the origin of $f(U)$.

Also, from the equation 2.62, the parameters $\mathrm{C}_1, \mathrm{C}_2$ and a are describe target attributes like I and E_P.

Additionally, E_P is influenced by target features like ionization potential and molecule size and shape. At elevated energy levels, the non-continuous excitation mechanisms, predominantly influenced by dipole transitions, diminish in proportion to $\frac{\ln (U)}{U}$. The reduction of the function f(U) in extensive energy intervals must likewise correspond to $\frac{\ln (U)}{U}$.

Therefore, we use three different criteria based on the ratio R to find these parameters

(1) R is zero at or below the ionization threshold, as no ionization occurs.

(2) At the peak energy E_P, follows the trend set by expression 2.59.

(3) For energies much higher than E_P, R approaches 1, which reflecting ionization is dominant.

This approach for determining the total ionization CSs is known as the "Complex Scattering Potential-ionization contribution". We have successfully validated it on several molecules, as discussed in the following chapters.

2.5 Approximations for charge density

The demonstrated effectiveness of the “SCOP” formalism for atomic systems has led us to explore its application to molecular targets. This formalism was originally designed for atomic systems, it necessitates several modifications to accommodate the complexities of molecular interactions. The following sections will detail these modifications. While various research groups [27,28] have concentrated on determining total and ionization CSs for electron impact on molecules, our research has focused on the simultaneous calculation of both the total (Q_T) and the ionization (Q_{ion}) CSs within a theoretical formalism. To extend these methods to polyatomic molecules, the development of appropriate approximation techniques is required. We begin by introducing the “Additivity Rule (AR)” [20] as a foundational approach for analyzing electron-molecule collision.

The “Additivity Rule (AR)” is a simplified, high-energy approach that assumes the total CSs of a molecule or atom can be determined by summing the total CSs of its individual atomic components. However, this approximation neglects the influence of molecular bonding, leading to inaccuracies. To address this limitation, the Modified Additivity Rule (MAR) was introduced, offering improved results over AR. Despite these advancements, MAR remains unreliable in certain cases. This shortcoming has motivated us to adopt a more robust and consistent method that provides greater accuracy while maintaining simplicity.

2.5.1 Additivity rule (AR)

The AR originates from the expansion of the high-energy “Independent Atom Model (IAM)” approximation [20,28,29]. IAM is based on two main assumptions:

1. Atoms in a molecule are treated separately, and ignoring the fact that they are bound together and the incident electron encounters the fields of other atoms.

2. There is no multiple scattering occurs, meaning that after scattering, the electron travels directly to the detector, with no further contact with other atoms in the molecule.

In the AR, all atomic CSs are derived individually and then merged under the specific condition. Let $Q(X)$, $Q(Y)$, and $Q(XY)$ are the relevant CSs for atom X, atom Y and XY molecule respectively.

$$Q(\mathrm{XY}) = Q'(\mathrm{X}) + Q'(Y) \tag{2.63}$$

A significant feature of the above equation indicates an advancement in the theoretical framework additive atomic cross-sections. Usually, the equation 2.63 as written for molecular cross sections is given as,

$$Q(M) = \sum_{i=1}^{n} Q'(X_i) \tag{2.64}$$

Here, $Q'(A_i)$ is the CSs for individual atom in investigated molecule, and n represents the total no. of individual atoms.

(i) Simple AR

The expression 2.65 demonstrates the application of the "simple additivity rule (AR)" when Q' solely represents the complete CSs of an atom.

$$Q(\mathrm{XY}) = Q(\mathrm{X}) + Q(\mathrm{Y}) \tag{2.65}$$

This seems to be valid for molecules with increased atomic bond length and applicable at intermediate and high energies. However, the results appear quite overestimating at lower energy.

(ii) Modified Additivity Rule (MAR)

In this case of the Modified Additivity Rule (MAR), specific cross sections (CSs) are modified to account for molecular properties, such as molecular structure and ionization potential. Various forms of MAR have been discussed in the previous work, that is relevant with various

feature of the molecule consider into the modified version of the AR. The MAR method for calculating the total ionization CSs of a molecule is structured as follows [30]:

The ionization potential is a key factor when calculating a molecule's total ionization cross section, surpassing other parameters in importance. In the "Modified Additivity Rule (MAR)", atomic inelastic CSs are recalculated by replacing each atom's ionization potential with that of the entire molecule. For instance, the total CSs of N_2 is determined by summing the individual oxygen atomic cross sections, each calculated using the ionization potential of N_2. The "CSP-ic" methodology is then applied to estimate Q_{ion}. Molecular geometry, such as bond lengths and angles, also influences cross section calculations. This method offers a reliable means of estimating Q_{ion} for larger biological molecules [31], with additional variants of MAR available in the literature [29,32,33].

2.6 2 parameters Semi Empirical Method (2p – SEM)

In the earlier research, the consequence of energy reliance of the Q_T for the intermediate [38,39] and high [40,41] was examined and the formula was suggested as,

$$Q_T = A/E^B \tag{2.66}$$

The parameter A in the equation 2.66 is influenced by molecular characteristics like size and polarizability. For high energies (above 500 eV), the value of B is approximately 0.7, as suggested by K. N. Joshipura [40] and Garcia G. [41] for tiny molecular species (n_e =10 to 22). This study extends this formula to larger molecules, whose n_e are between 55 to 95.

Furthermore, the relationship between Q_T and incident energy (E_i) exhibits variability across various energy domains. The research presents two separate formulations for intermediate (50 to 500 eV) and high energy (above 500 eV) ranges concerning these intricate, larger molecular systems.

In table 2.6 we show A and B, demonstrating a stable value of B (around 0.56) across the entire set of molecules.

The calculations indicate that the total CSs are dynamic and its energy dependency is similar to the one observed in previous work of Nishimura & Tawara [38] for the 50-500 eV as,

$$Q_T = A/\sqrt{E} \tag{2.73}$$

Thus, the A is different for each target and it is dependents on the number of electrons (n_e) of the target.

Table 2.4 Calculated A and B

Targets	***Parameters***	
	A	***B***
$\mathbf{C_5H_5N_5}$	46.53	0.58
$\mathbf{C_5H_5N_5O}$	54.79	0.56
$\mathbf{C_5H_6N_2O_2}$	43.66	0.57
$\mathbf{C_4H_5N_3O}$	34.68	0.56
$\mathbf{C_4H_4N_2O_2}$	34.56	0.53

As shown in figures 2.3 and 2.4 for $50 < E_i < 500\ eV$ and $E_i > 500\ eV$, respectively, we have plotted the graph of parameter "A" versus number of electrons (n_e) to obtain the following expression.

$A(n_e) = n_e - 23.54$ (Correlation r = 99%)

The aforementioned formula illustrates the linear correlation seen between parameter A and number of electrons (n_e) in figure 2.3.

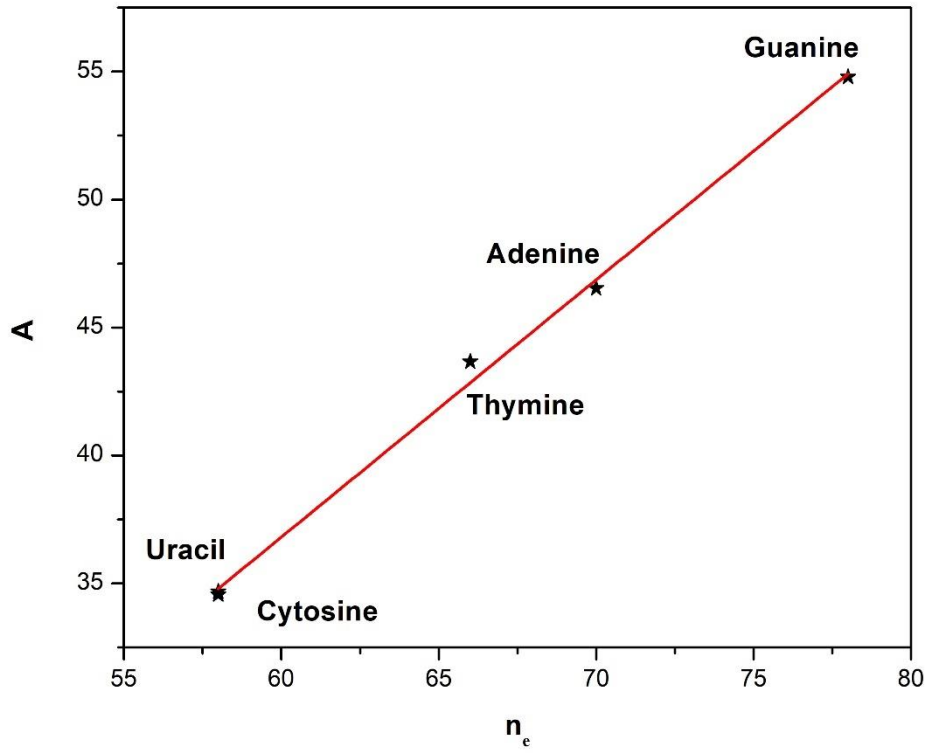

Figure 2.3 *"A" vs "n_e"* ($50\ eV < E_i < 500\ eV$)

Nonetheless, the precision of this estimation may be enhanced for the objective by contrasting the actual measurements of 'A' (as shown in Table 2.6) with those forecasted by equation 2.67 for a specific n_e.

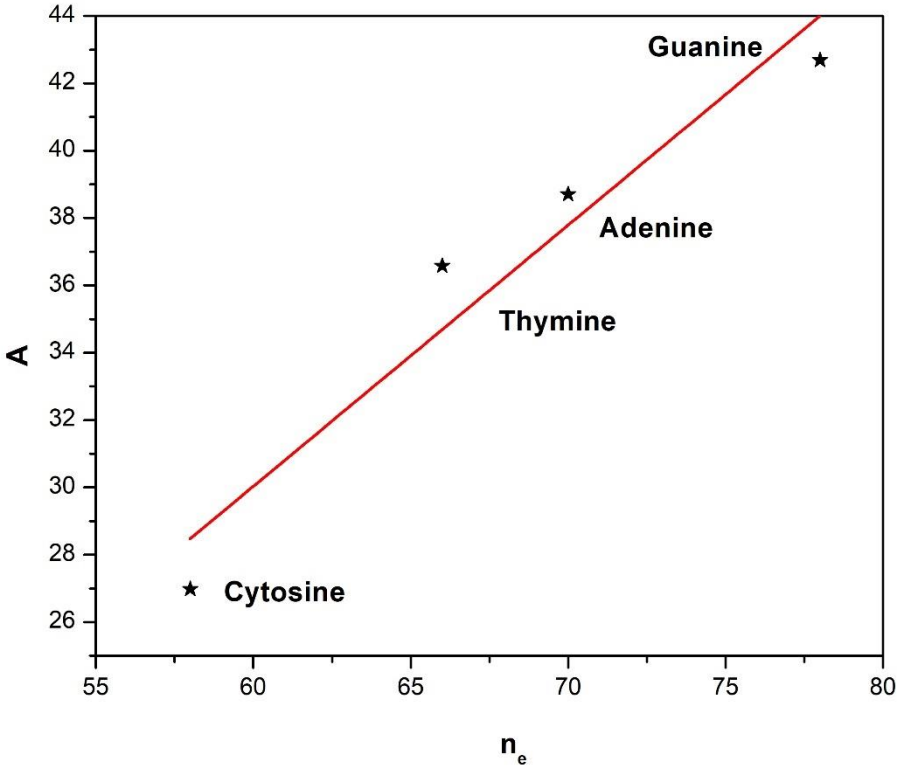

Figure 2.4 ***"A" vs "n_e" ($E_i > 500$ eV)***

We have observed a correlation between the deviation (A - A(n_e)) and the target polarizability (α). The expression is,

$$A - A(n_e) = -0.003 * \alpha + 0.63 \tag{2.68}$$

Consequently, based on equations 2.66, 2.67, and 2.68, a two-parameter for Q_T equation can be derived for the energy range of 50 eV to 500 eV,

$$Q_T(E, n_e, \alpha) = \frac{n_e - 0.003 * \alpha - 22.91}{E^{0.56}} \tag{2.69}$$

The equation with two parameters of Q_T as a function of α and n_e has similarly been established through this approach for incident energy exceeding 500 eV.

$$Q_T(E, n_e, \alpha) = \frac{0.776 * n_e + 0.016 * \alpha - 17.88}{E^{0.77}} \quad (2.70)$$

It is noted that the value of B is 0.56 for the lower range and 0.77 for the upper range of the incident energy. The equations 2.69 and 2.70 provide the two-parameter formulations for impact energy within the bounds of 50 eV < E_i < 500 eV and 50 eV < E_i < 500 eV, facilitating the calculation of Q_T across the entire energy spectrum being analyzed.

2.7 Estimation of dielectric constant, ε

The dielectric constant (ε) of molecules plays a crucial role in enhancing energy storage systems, developing superior insulation materials, creating innovative electronic devices, and optimizing electrical characteristics.

The expression of Clausius Mosotti [43] typically written as,

$$\frac{\varepsilon - 1}{\varepsilon + 2} = \frac{4\pi}{3} * N * \alpha \quad (2.71)$$

Where, "α" is the "dipole polarizability" and "N" is the "number density".

The number density can be estimated through below expression [44]

$$N = \frac{N_A * \rho}{M} \quad (2.72)$$

Here, "ρ" =density, "N_A" =Avogadro number and "M" =molar mass of the molecule.

$$Q_{ion(\mathrm{m})} = \frac{e}{4\varepsilon_o}\sqrt{\frac{\alpha}{\Delta}} \quad (2.73)$$

Harland proposed that the maximum ionization ($Q_{ion(max)}$) CSs have a qualitative dependency nature, with its dipole polarizability (α) [45],

In this work, two mathematical equations for the dielectric constant (ε) were obtained through the $Q_{ion(max)}$ on α and ε, as presented in equation 2.73. The first equation of the $Q_{ion(max)}$, was derived by integrating the relationship between the $Q_{ion(max)}$ with α.

The expression of Clausius-Mosotti is given as,

$$\frac{\varepsilon - 1}{\varepsilon + 2} = C \cdot (Q_{ion}(max))^2 N\Delta \tag{2.74}$$

Here, $C = \frac{64\pi}{3}\left(\frac{\varepsilon_o}{e}\right)^2$

The formula of Onsager given for liquid [46] very well is described by,

$$\frac{\varepsilon - 1}{\varepsilon + 2} = \frac{4\pi}{3}\alpha N + \frac{(\varepsilon - \varepsilon_\infty)(2\varepsilon + \varepsilon_\infty)}{\varepsilon(\varepsilon_\infty + 2)^2} \tag{2.75}$$

In the context of this aqueous phase study, this equation is considered more suitable. Additionally, we propose an equation for the ε as a function of $Q_{ion(max)}$:

$$\frac{\varepsilon - 1}{\varepsilon + 2} = C \cdot \left(Q_{ion(max)}\right)^2 N\Delta + \frac{(\varepsilon - \varepsilon_\infty)(2\varepsilon + \varepsilon_\infty)}{\varepsilon(\varepsilon_\infty + 2)^2} \tag{2.76}$$

Where, the dielectric constant corresponding to high frequency is given by ε_∞.

2.8 Chapter summary

The present chapter describes various theoretical methodology which is adopted for the calculation of varieties of electron scattering cross sections. For all total cross sections Q_{inel}, Q_{el} and Q_T, our SCOP (Spherical Complex Potential method) methodology yields results that are comparatively good. Using the CSP-ic approach, the theoretical Q_{inel} is divided into Q_{ion} and $\sum Q_{exc}$. In theory, all permitted ionizations caused by incident electrons are included in the current total ionization cross sections, which are simply expressed as Q_{ion}. Compared to other theoretical methods, our method for calculating Q_{ion} is simpler. Also, we have developed a novel approach for the calculation of total cross sections for complex molecules 55<Z<95,

whose experiment is difficult to perform. In earlier research, it provided a fair amount of agreement for a large number of atoms and molecules.

2.9 Bibliography

[1] B. H. Bransden and C. J. Joachain, *Physics of Atoms and Molecules (2nd Edition)*, **1112** (2003).

[2] E. Clementi and C. Roetti, *Roothaan-Hartree-Fock Atomic Wavefunctions: Basis Functions and Their Coefficients for Ground and Certain Excited States of Neutral and Ionized Atoms, Z≤54*, At Data Nucl. Data Tables **14**, 177 (1974).

[3] C. F. Bunge, J. A. Barrientos, and A. V. Bunge, *Roothaan-Hartree-Fock Ground-State Atomic Wave Functions: Slater-Type Orbital Expansions and Expectation Values for Z = 2-54*, At Data Nucl Data Tables **53**, 113 (1993).

[4] M. Swadia, Theoretical Investigation of Electrons with Molecules of Biological and Industrial Relevance through Wide Energy Range (2017).

[5] H. L. Cox and R. A. Bonham, *Elastic Electron Scattering Amplitudes for Neutral Atoms Calculated Using the Partial Wave Method at 10, 40, 70, and 100 KV for Z = 1 to Z = 54*, J Chem Phys **47**, 2599 (1967).

[6] B. K. Antony, Theoretical Study of Electron Collisions and Ionization of Atoms Molecules and Clusters, (2005).

[7] F. Salvat, J. D. Martnez, R. Mayol, and J. Parellada, *Analytical Dirac-Hartree-Fock-Slater Screening Function for Atoms (Z=1–92)*, Phys Rev A **36**, 467 (1987).

[8] S. Hara, Hara, and Shunsuke, *The Scattering of Slow Electrons by Hydrogen Molecules*, J. Phys. Soc. Jpn. **22**, 710 (1967).

[9] M. E. Riley and D. G. Truhlar, *Approximations for the Exchange Potential in Electron Scattering*, J Chem Phys **63**, 2182 (1975).

[10] C. J. Joachain, *Quantum Collision Theory*, **710** (1975).

[11] R. Buckingham, *The Quantum Theory of Atomic Polarization. I. Polarization by a Uniform Field*, Proceedings of The Royal Society A: Mathematical, Physical and Engineering Sciences **160**, 94 (1937).

[12] S. P. Khare and D. Raj, *Elastic Scattering of Electrons by O_2 and CO_2 Molecules at Intermediate Energies*, Indian Journal of Pure and Applied Physics **20**, 538 (1982).

[13] C. C. Lin and L. W. Anderson, Adv. At. Molec. Opt. Phys. 29, **1** (1992).

[14] Leonard I. Schiff, *Quantum Mechanics*, **544** (1968).

[15] A. Reitan, *Potential and Glauber Scattering of Electrons by Complex Atoms*, Phys Scr **22**, 615 (1980).

[16] A. E. S. Green, D. E. Rio, and T. Ueda, *Analytic Velocity-Dependent Potential for Bound and Scattering States of Electrons and Atoms*, Phys Rev A **24**, 3010 (1981).

[17] G. Staszewska, D. W. Schwenke, D. Thirumalai, and D. G. Truhlar, *Quasifree-Scattering Model for the Imaginary Part of the Optical Potential for Electron Scattering*, Phys Rev A **28**, 2740 (1983).

[18] G. Staszewska, D. W. Schwenke, and D. G. Truhlar, *Investigation of the Shape of the Imaginary Part of the Optical-Model Potential for Electron Scattering by Rare Gases*, Phys Rev A **29**, 3078 (1984).

[19] F. Blanco and G. García, *Improvements on the Quasifree Absorption Model for Electron Scattering*, Phys Rev A **67**, 022701 (2003).

[20] K. N. Joshipura and M. Vinodkumar, *Electron Scattering Cross Sections with HF, OH, NH and CH Molecules*, Physics Letters, **224**, 361 (1997).

[21] K. N. Joshipura, M. Vinodkumar, C. G. Limbachiya, and B. K. Antony, *Calculated Total Cross Sections of Electron-Impact Ionization and Excitations in Tetrahedral [Formula Presented] and [Formula Presented] Molecules*, Phys Rev A **69**, 6 (2004).

[22] W. Hwang, Y. K. Kim, and M. E. Rudd, *New Model for Electron-impact Ionization Cross Sections of Molecules*, J Chem Phys **104**, 2956 (1996).

[23] H. Deutsch, K. Becker, S. Matt, and T. D. Märk, *Theoretical Determination of Absolute Electron-Impact Ionization Cross Sections of Molecules*, Int J Mass Spectrom **197**, 37 (2000).

[24] C. Limbachiya, M. Vinodkumar, M. Swadia, K. N. Joshipura, and N. Mason, *Electron-Impact Total Cross Sections for Inelastic Processes for Furan, Tetrahydrofuran and 2,5-Dimethylfuran*, Mol Phys **113**, 55 (2015).

[25] J. E. Turner, H. G. Paretzke, and R. N. Hamm, *Comparative Study of Electron Energy Deposition and Yields in Water in the Liquid and Vapor Phases*, Radiat Res **92**, 47 (1982).

[26] K. N. Joshipura and Minaxi Vinodkumar, Phys. Letts. A **41**, 361 (1997).

[27] S. P. Khare, *Introduction to the Theory of Collisions of Electrons with Atoms and Molecules*, (2001).

[28] L. G. Christophorou, *Electron-Molecule Interactions and Their Applications. Volume 2*, (1984).

[29] A. Jain and S. S. Tayal, *Elastic Scattering of Electrons by HCN Molecules in a Two-Potential Hybrid Approach at 21.6-700 EV*, Journal of Physics B: Atomic and Molecular Physics **17**, L37 (1984).

[30] Chetan G. Limbachia, *Collision Interactions of Electrons with Atomic and Molecular Targets- a Theoretical Study*, Ph.D. thesis, Sardar Patel University, India (2005).

[31] B. K. Antony, K. N. Joshipura, and N. J. Mason, *Electron Impact Ionization Studies with Aeronomic Molecules*, Int J Mass Spectrom **233**, 207 (2004).

[32] H. Deutsch, C. Cornelissen, L. Cespiva, V. Bonacic-Koutecky, D. Margreiter, and T. D. Märk, *Total Electron Impact Ionization Cross Sections of Free Molecular Radicals: The Failure of the Additivity Rule Revisited*, Int J Mass Spectrom Ion Process **129**, 43 (1993).

[33] H. Deutsch, K. Becker, and T. D. Märk, *A Modified Additivity Rule for the Calculation of Electron Impact Ionization Cross-Section of Molecules ABn*, Int J Mass Spectrom Ion Process **167–168**, 503 (1997).

[34] R. F. W. Bader, *Atoms in Molecules: A Quantum Theory, Oxford University Press*, 438 (1990).

[35] G. N. (George N. Watson, *A Treatise on the Theory of Bessel Functions*, 804 (1966).

[36] I. S. Gradštejn, J. M. Ryžik, Ju. V. Geronimus, M. Yu. Cejtlin, and Alan. Jeffrey, *Table of Integrals, Series, and Products*, (1965).

[37] M. Vinodkumar, K. Korot, and P. C. Vinodkumar, *Complex Scattering Potential – Ionization Contribution (CSP-ic) Method for Calculating Total Ionization Cross Sections on Electron Impact*, The European Physical Journal D 2010 59:3 **59**, 379 (2010).

[38] H. Nishimura and H. Tawara, *Some Aspects of Total Scattering Cross Sections of Electrons for Simple Hydrocarbon Molecules*, Journal of Physics B: Atomic, Molecular and Optical Physics **24**, L363 (1991).

[39] A. Zecca, G. P. Karwasz, and R. S. Brusa, Phys. Rev. A, 45(5), (1992).

[40] K. N. Joshipura and M. Vinodkumar, *Cross Sections and Other Parameters of E- - H2O Scattering (Ei≥50eV)*, Pramana - Journal of Physics **47**, 57 (1996).

[41] G. García and F. Manero, *Correlation of the Total Cross Section for Electron Scattering by Molecules with 10-22 Electrons, and Some Molecular Parameters at Intermediate Energies*, Chem Phys Lett **280**, 419 (1997).

[42] M. Vinodkumar, C. Limbachiya, M. Barot, A. Barot, and M. Swadia, *Electron Impact Total Cross Sections for Components of DNA and RNA Molecules*, Int J Mass Spectrom **360**, 1 (2014).

[43] C. Kittel and D. F. Holcomb, *Introduction to Solid State Physics*, 8th ed., Vol. 35 (1967).

[44] de P. J. Atkins P, Atkins PW, *Atkins' Physical Chemistry* (Oxford university press, 2014).

[45] P. W. Harland and C. Vallance, *Ionization Cross-Sections and Ionization Efficiency Curves from Polarizability Volumes and Ionization Potentials*, Int J Mass Spectrom Ion Process **171**, 173 (1997).

[46] L. Onsager, *Electric Moments of Molecules in Liquids*, J Am Chem Soc **58**, 1486 (1936).